

BACKSCATTER LASER DEPOLARIZATION STUDIES OF SIMULATED STRATOSPHERIC
AEROSOLS: CRYSTALLIZED SULFURIC ACID DROPLETS

FINAL REPORT

Prepared for

National Aeronautics and Space Administration
Grant No. NAG-1-686
(2 June 1986 - 1 June 1988)

Prepared by

Kenneth Sassen, Hongjie Zhao and Bing-Kun Yu

Meteorology Department
University of Utah
Salt Lake City, Utah 84112

(NASA-CR-183387) BACKSCATTER LASER
DEPOLARIZATION STUDIES OF SIMULATED
STRATOSPHERIC AEROSOLS: CRYSTALLIZED
SULFURIC ACID DROPLETS Final Report, 2 Jun.
1986 - 1 Jun. 1988 (Utah Univ.) 20 p

N89-13111

G3/46 Unclass
C172882

BACKSCATTER LASER DEPOLARIZATION STUDIES OF SIMULATED STRATOSPHERIC

AEROSOLS: CRYSTALLIZED SULFURIC ACID DROPLETS

Kenneth Sassen, Hongjie Zhao and Bing-Kun Yu*

Department of Meteorology
University of Utah
Salt Lake City, Utah 84112

ABSTRACT

The optical depolarizing properties of simulated stratospheric aerosols were studied in laboratory laser (0.633 μm) backscattering experiments for application to polarization lidar observations. Clouds composed of sulfuric acid solution droplets, some treated with ammonia gas, were observed during evaporation. The results indicate that the formation of minute ammonium sulfate particles from the evaporation of acid droplets produces linear depolarization ratios of $\delta \approx 0.02$, but $\delta \approx 0.10-0.15$ are generated from aged acid cloud aerosols and acid droplet crystallization effects following the introduction of ammonia gas into the chamber. It is concluded that partially crystallized sulfuric acid droplets are a likely candidate for explaining the lidar $\delta \approx 0.10$ values that have been observed in the lower stratosphere in the absence of the relatively strong backscattering from homogeneous sulfuric acid droplet ($\delta \approx 0$) or ice crystal ($\delta \approx 0.5$) clouds.

*Current Address: Department of Physics, Shanghai University of Science and Technology, Shanghai, People's Republic of China

1. Introduction

In recent years, increasing evidence has emerged that the clouds of the earth's stratosphere are composed of rather exotic aerosols. In view of the fact that atmospheric physicists have traditionally placed the greatest emphasis on the water and ice particle microphysical processes that lead to precipitation, a perspective based on extraterrestrial atmospheres seems more appropriate for understanding these tenuous clouds. Nonetheless, the combined data obtained from balloon-borne sampling devices, airborne and ground-based lidar probing, and satellite-based passive remote sensing observations have indicated that stratospheric clouds may have a significant effect on climate and atmospheric processes. Both volcanically-injected aerosol clouds¹ and polar stratospheric clouds² have been linked to climatic perturbations, and it has also been theorized that stratospheric cloud formation and ozone depletion during the polar night are interrelated.³

Much of the recent evidence concerning the composition of stratospheric cloud particles has been inferred from polarization lidar observations, which provide indications of particle shape. In combination with atmospheric chemistry model findings, it has been possible to arrive at several candidates for aerosol species that could account for the lidar depolarization data and satisfy the basic atmospheric/chemical requirements. The chief candidate is an aqueous solution of concentrated sulfuric acid ($\sim 75\% \text{H}_2\text{SO}_4$), the same material that comprises the clouds of Venus. In the case of clouds of volcanic origin, sulfur dioxide gas injected into the stratosphere is believed to become photo-oxidized and combine with water vapor, and possibly particulates, to form clouds of sulfuric acid droplets following a major eruption. Such clouds display very low amounts of laser linear depolarization consistent with the single-scattering behavior of spherical particles.⁴ Other lidar measurements suggest that

stratospheric ice crystal clouds, which yield the considerably higher depolarizations typical of cirrus clouds in the upper troposphere, also occur in both the midlatitude⁴ and polar regions.^{5,6} Finally, there is a class of stratospheric observations that reveal lidar depolarizations that are somewhat higher than those for spherical particles, but significantly less than expected for typical ice crystals. This depolarizing behavior could perhaps be attributed to small (i.e., relative to the laser wavelength) nonspherical particulates, near-spherical frozen droplets, or a mixture of spherical and nonspherical particles. These conditions appear to prevail between volcanic eruptions and in Type I polar stratospheric clouds,⁷ and may in some cases be associated with the decay of volcanic aerosol clouds. Various suggested compositions for these clouds include ammonium sulfate particles,⁴ and frozen nitric acid⁷ and sulfuric acid⁸ particles.

Reported here are the results of a laboratory investigation of the backscatter depolarizing properties of simulated stratospheric aerosols composed of sulfur compounds. The measurements were obtained with a cw laser-lidar analog device for application to the interpretation of polarization lidar measurements of the stratosphere, although in the current experimental phase actual stratospheric temperatures and pressures were not simulated. Nonetheless, the results can be interpreted as lending support to the importance of sulfur compound aerosols as a cloud forming component of the stratosphere.

2. Experimental Design

The lidar-analog laboratory scattering device consists of a helium-neon (0.633 μm wavelength) laser and a dual-polarization receiver of a design described previously.⁹ The vertically polarized laser beam is directed through the cloud chamber by means of a 45° mirror, which preserves the incident beam

polarization properties, directly in front of the receiver lens. Cloud extinction is monitored with reference to the laser output using a power meter located ~2 m from the center of the scattering volume to help exclude forward scattered radiation. Although single scattering in the exact backward direction is not measured due to the obstruction caused by the mirror, the receiver optics are designed to limit the cone of backscattered light from the scattering volume to an angle of $\leq 178^\circ$ with respect to the incident direction.

Data handling is accomplished with a microcomputer-based system. The two-channel backscatter signals, corresponding to the vertical E_{\parallel} and horizontal E_{\perp} polarization components, are processed after amplification using picoameters that have been calibrated over a four-decade range to ensure accuracy over a large signal dynamic range. The stored data points typically represent an average of 250 samples (of 0.1 s duration) obtained at 25 s intervals. Calibrations of the receiver channel gains are performed by viewing an unpolarized target consisting of a diffused light source, and the receiver polarization orientation is aligned with that of the source by minimizing the backscattered depolarization measured in stable water droplet clouds. After adjusting the backscattered signals for the effects of background signal voltages, including background molecular/aerosol scattering, the lidar linear depolarization ratio is calculated from $\delta = E_{\perp} / E_{\parallel}$. Since the strengths of the background signals resulting from scattering off the rear cloud chamber window and the power meter assembly change with cloud optical thickness during an experiment, their relative contributions are adjusted by taking into account the two-way extinction of the incident and background radiation through the cloud.

The cloud chamber, which has a total volume of 50 liters and a height of 1.1 m, has been constructed out of high vacuum stainless steel components to accommodate a wide range of planetary atmospheric conditions. The enlarged

bottom bay of the chamber contains two opposed viewports for laser scattering studies, providing a scattering volume length of 0.6 m. The viewports are heated to prevent condensation on the window surfaces. To reduce the signal noise associated with the use of windows, the front window is positioned normal to the laser beam direction, such that the retroreflection is directed back to the mirror and into the laser, while the rear window is offset at a large angle to the incident beam to divert the surface reflection to the side of the viewport. The chamber is fitted with connections for vacuum, regulated gas delivery, and vent systems. Samples of cloud particles collected by sedimentation during an experiment can be obtained by means of a glass microscope slide injection device.

To produce the clouds, droplets generated with an ultrasonic nebulizer are introduced into the top of the chamber and allowed to settle into the scattering volume. Experiments have been performed with fluid samples of 40-45% sulfuric acid by weight in distilled water, and also for comparison using pure distilled water. Previous experience has shown that this cloud generating device produces water droplets with modal radii between 5.0 and 10.0 μm . Typically, the chamber is allowed to become filled with droplets until the cloud optical thickness $\tau \geq 1.0$, and then dry nitrogen gas is introduced at a flow rate of a few liters per minute to begin evaporating the droplets. Thereafter, the cloud optical thickness gradually decreases in response to the combined effects of droplet evaporation and the flushing of particles from the chamber. After a sulfuric acid cloud experiment, the chamber is evacuated to remove residual particles and gases, and room air is reintroduced into the chamber. However, for some tests, the residual aerosol was left in the chamber and allowed to age prior to water cloud formation, and in other experiments small amounts of ammonia gas (typically $<0.1 \text{ l}$) were introduced into sulfuric acid clouds to promote acid droplet

crystallization.

3. Experimental Results

a. Acid Droplet Single and Multiple Scattering

It is a fundamental scattering principle that no depolarization of an incident electromagnetic wave is produced in the exact backscatter direction from particles that are spherical and optically homogeneous. However, as amply illustrated by polarization lidar studies of water droplet clouds,¹⁰ dense assemblies of spherical scatterers induce a depolarized component as a consequence of the multiple scattering activity viewed by the finite field-of-view of the receiver. This depolarizing effect is in essence cumulative as the laser pulse penetrates into a dense water cloud, such that lidar δ values gradually increase with increasing optical depth. Aside from the lidar design factors, the amount of depolarization generated is related to the ensemble azimuthal angular scattering pattern,¹¹ which is a function of the radius and refractive index of cloud droplets. Thus, although no backscatter depolarization is to be expected for a spherical droplet regardless of the material's composition, the multiple scatter depolarizing behavior of sulfuric acid solution droplets, say, could be dissimilar from that of pure water droplets.

Compared in Fig. 1 are depolarization and relative returned (parallel-polarized) laser energy data for evaporating sulfuric acid and pure water droplet clouds. These curves represent the average of five experiments for each cloud type, with the standard deviations given as the bars. The data are shown as a function of cloud optical thickness τ , from which the average cloud extinction coefficient σ can be derived by dividing τ by the 0.6 m cloud path length. Interestingly, although the dependence of multiple-scattering induced depolarization on optical thickness is similar for the two cloud types, the

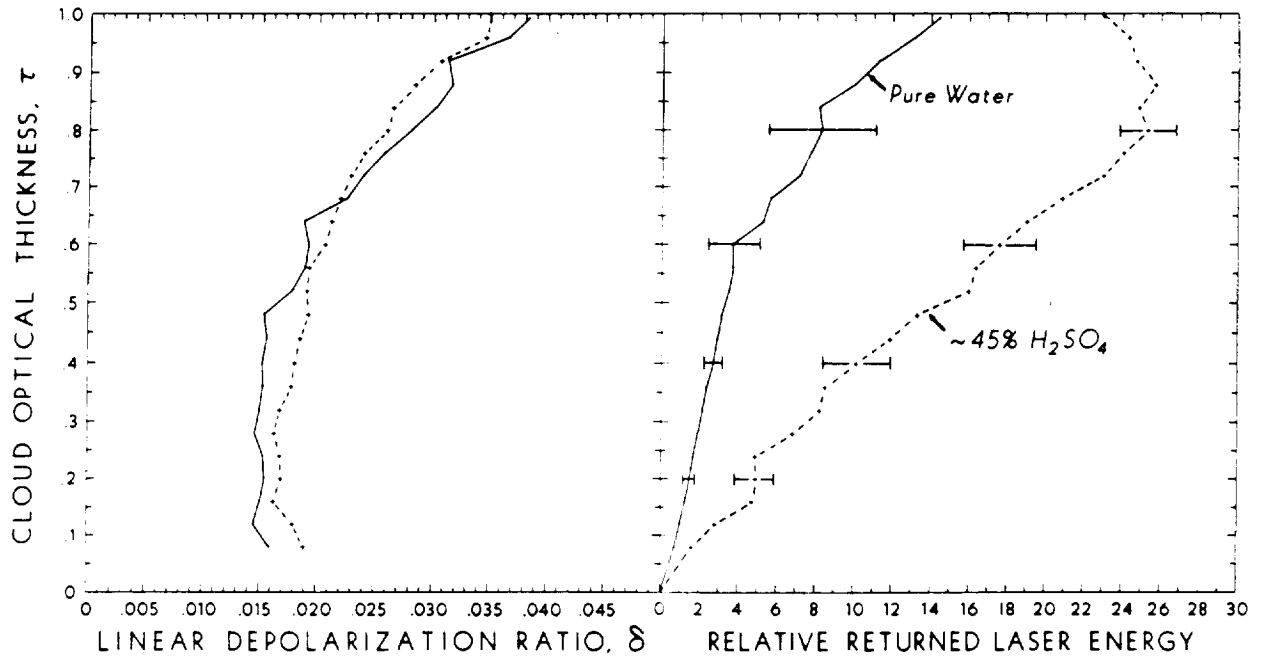


Fig. 1 Results of typical experiments for evaporating pure water and ~45% sulfuric acid solution droplet clouds in terms of the linear depolarization ratio (left) and relative backscattered laser energy (right, given in arbitrary units).

sulfuric acid cloud clearly backscatters more energy. As indicated by the Mie scattering simulations given in Fig. 2, this latter finding is related to the greater single backscattering efficiency of scatterers with the increased refractive index associated with acid solution drops, although the observed differences are stronger than would be anticipated from single scattering alone. It can also be noted that, for low values of τ , the water cloud δ tend to assume a constant value of -0.015 , while acid cloud depolarization is slightly higher and, in many cases, δ actually increase somewhat as the acid cloud finally dissipates. This behavior is consistent with the formation of inhomogeneous or nonspherical aerosols from the evaporating particles either through particulate scavenging or reaction product growth, as examined below.

b. Crystallized Droplet Scattering

As discussed, for example, by Rubel and Gentry,¹² reaction products resulting from gaseous diffusion to acid droplets can lead to particle crystallization at a rate dependent on drop size and reacting gas partial pressure. As already noted, and as shown by the "+" symbols in Figs. 3 and 4, the slight depolarization increases often measured in dissipating sulfuric acid clouds may indicate the development of particle inhomogeneities due to the absorption of a reactive gas. Presumably, ammonia is the reactive gas, and ammonium sulfate is the reaction product. However, the maximum δ values of -0.02 in Figs. 3-4 for the evaporated acid droplets suggest that either the scatterers are spherical but inhomogeneous haze particles, or dry particles that are small relative to the laser wavelength. In other words, reactive gases absorbed over the relatively short life cycle of an acid cloud in the laboratory environment are insufficient to generate large nonspherical aerosols, which could be expected to produce more significant depolarization. This implies that higher δ values might be encountered if the concentration of reactive gas species, or the time allowed

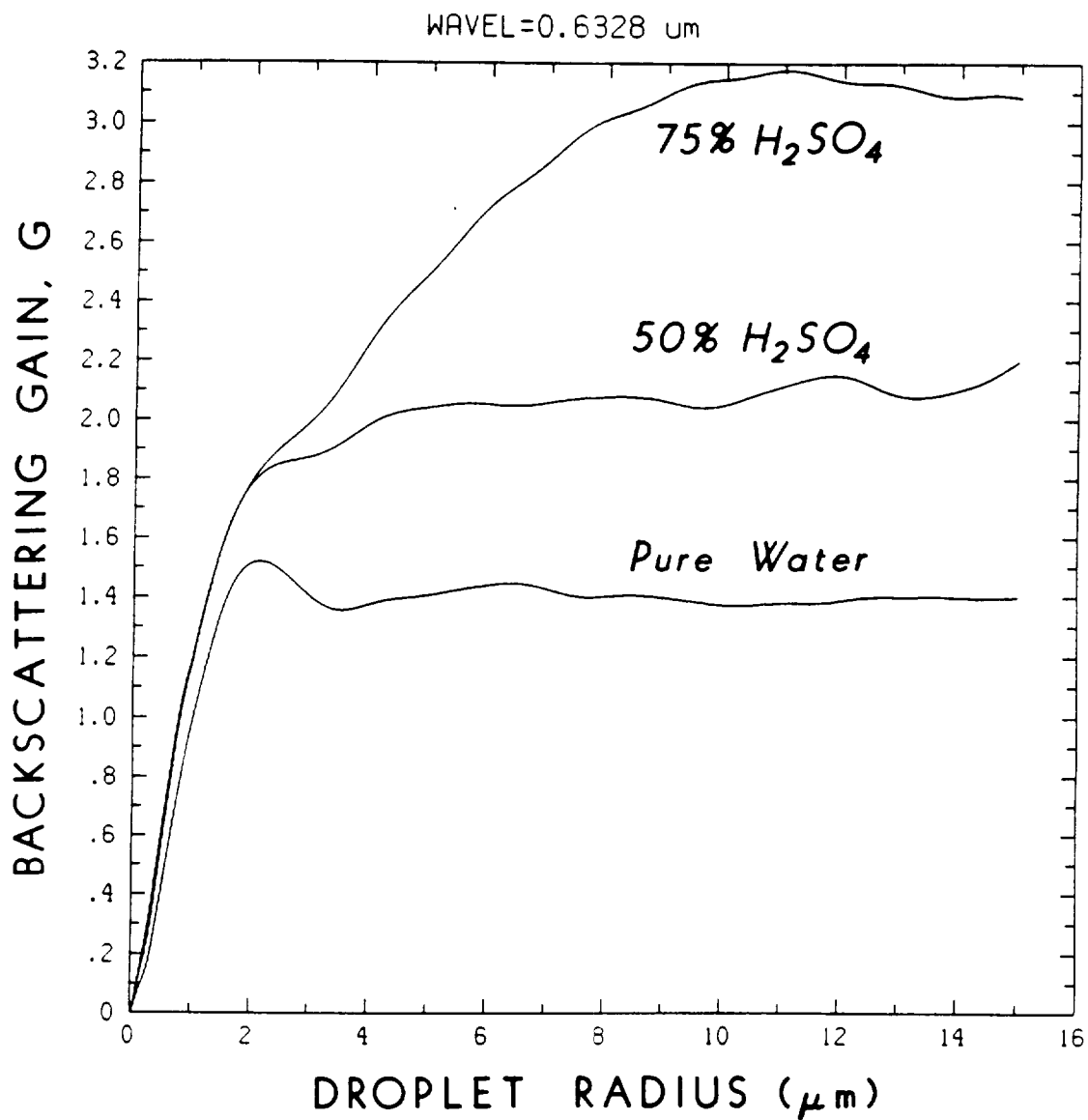


Fig. 2 Mie scattering predictions of the backscattering gain G for droplets of the indicated compositions, using refractive indices weighed according to the $n = 4/3 - i0$ and $1.43 - i2.5 \times 10^{-8}$ values for pure water and sulfuric acid, respectively. Values of G , shown here after smoothing to remove resonances, tend to increase strongly with increasing acid content, whereas extinction cross sections are unaffected.

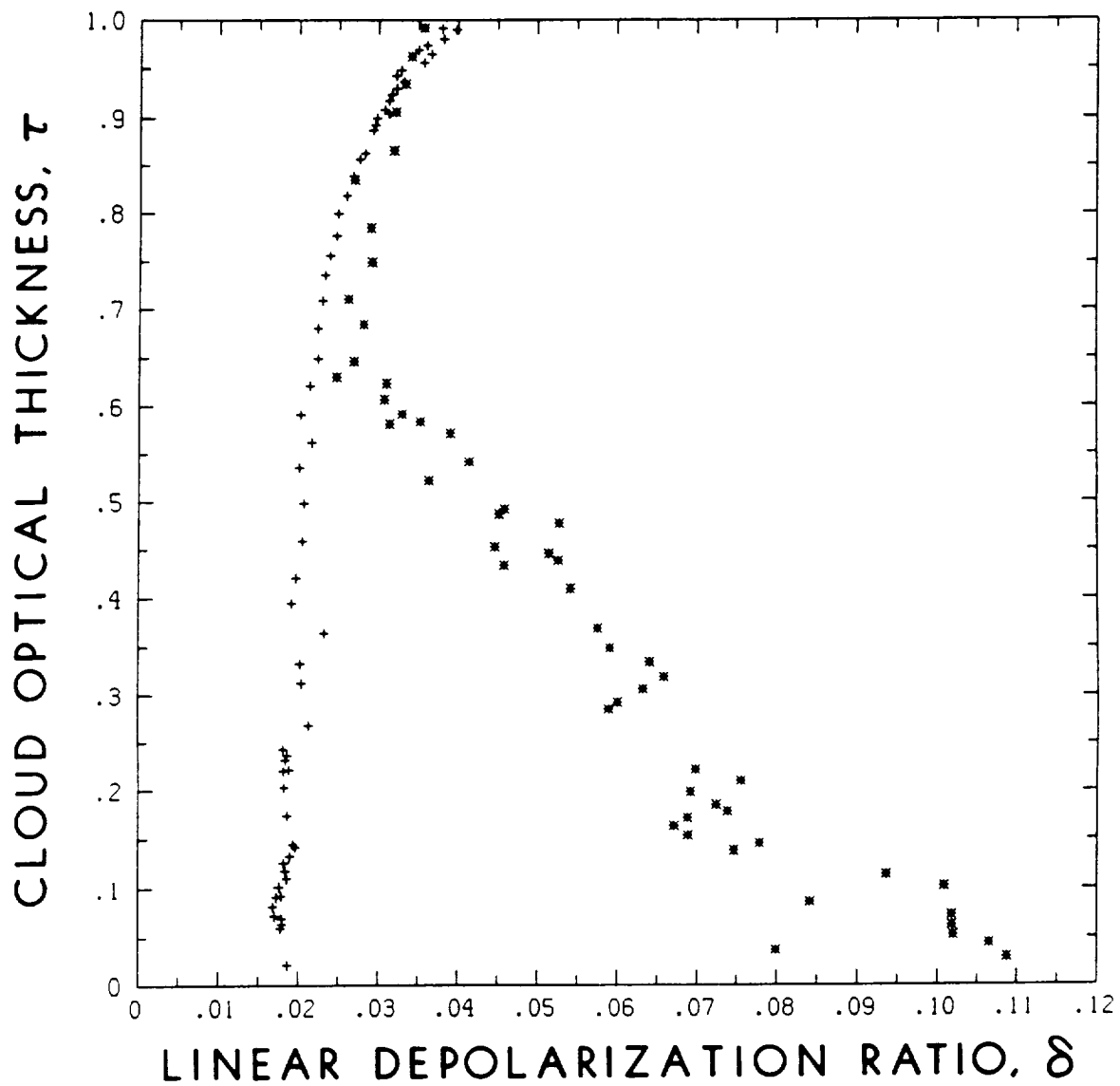


Fig. 3 The depolarizing behaviors of evaporating sulfuric acid solution droplets (+) and pure water droplets (*) contaminated by an aged aerosol from the evaporated acid cloud.

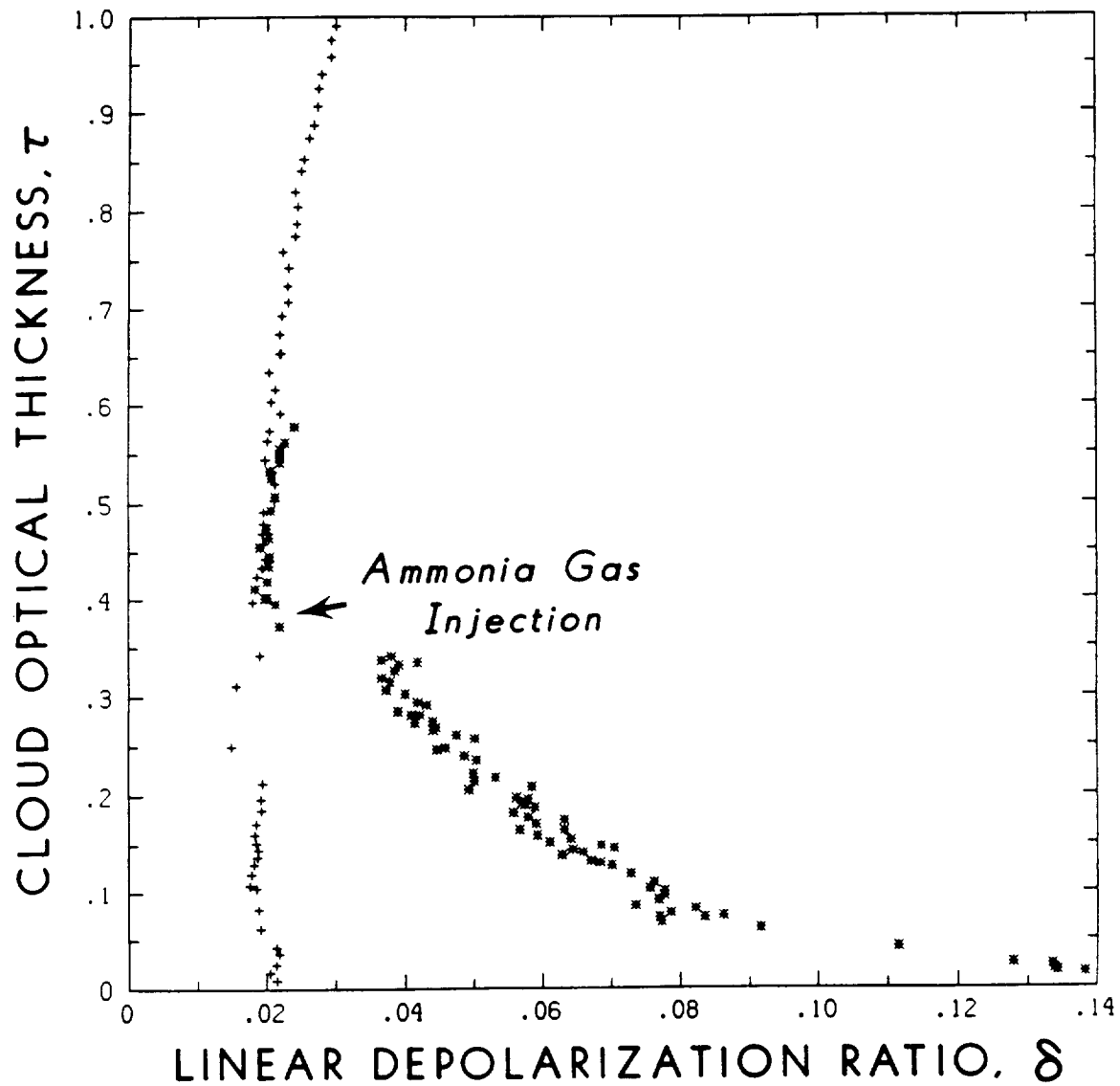


Fig. 4 Comparison of δ values from two sulfuric acid solution droplet clouds during evaporation. The "*" data points illustrate the effects of introducing a small amount of ammonia gas into the chamber (note arrow), which rapidly began crystallizing the acid droplets.

for the reaction, were to be increased.

The results shown by the "*" symbols in Figs. 3 and 4 demonstrate that this is indeed the case. In Fig. 3, an evaporated acid cloud (the "+" symbols) was not cleansed from the chamber and a subsequent experiment a day later using pure water droplets revealed a characteristic that is very similar to that of introducing a small quantity of ammonia gas directly into an acid cloud, as shown in Fig. 4. The mechanism responsible for the rather significant δ value increase during cloud evaporation is related to the crystallization process of comparatively large droplets. This is clearly a product of the increased rate of ammonia gas absorption by acid droplets in Fig. 4 (note arrow marking the time of gas injection into the evaporating cloud), whereas it can be concluded that the same crystallization feature present in Fig. 3 was induced by large cloud condensation nuclei (CCN) that were created from the coagulation and drop scavenging of the residual ammonium sulfate aerosols formed naturally overnight in the chamber. The enhanced δ values, after reaching peaks of 0.10-0.15, tend to display a decreasing trend during final cloud dissipation, which probably reflects the formation of dry aerosols and the sedimentation and removal of the larger particles.

4. Summary and Conclusions

Our interpretation of these findings from evaporating acid clouds is illustrated schematically in Fig. 5. Based on a large number of laser scattering experiments, we conclude that there are three basic depolarizing pathways associated with acid droplet evaporation, which reflect the varying influence of gaseous absorption and reaction product formation. The first path, in which reaction product formation is absent or negligible and evaporation is essentially complete, represents the classic dependence of multiple-scattering

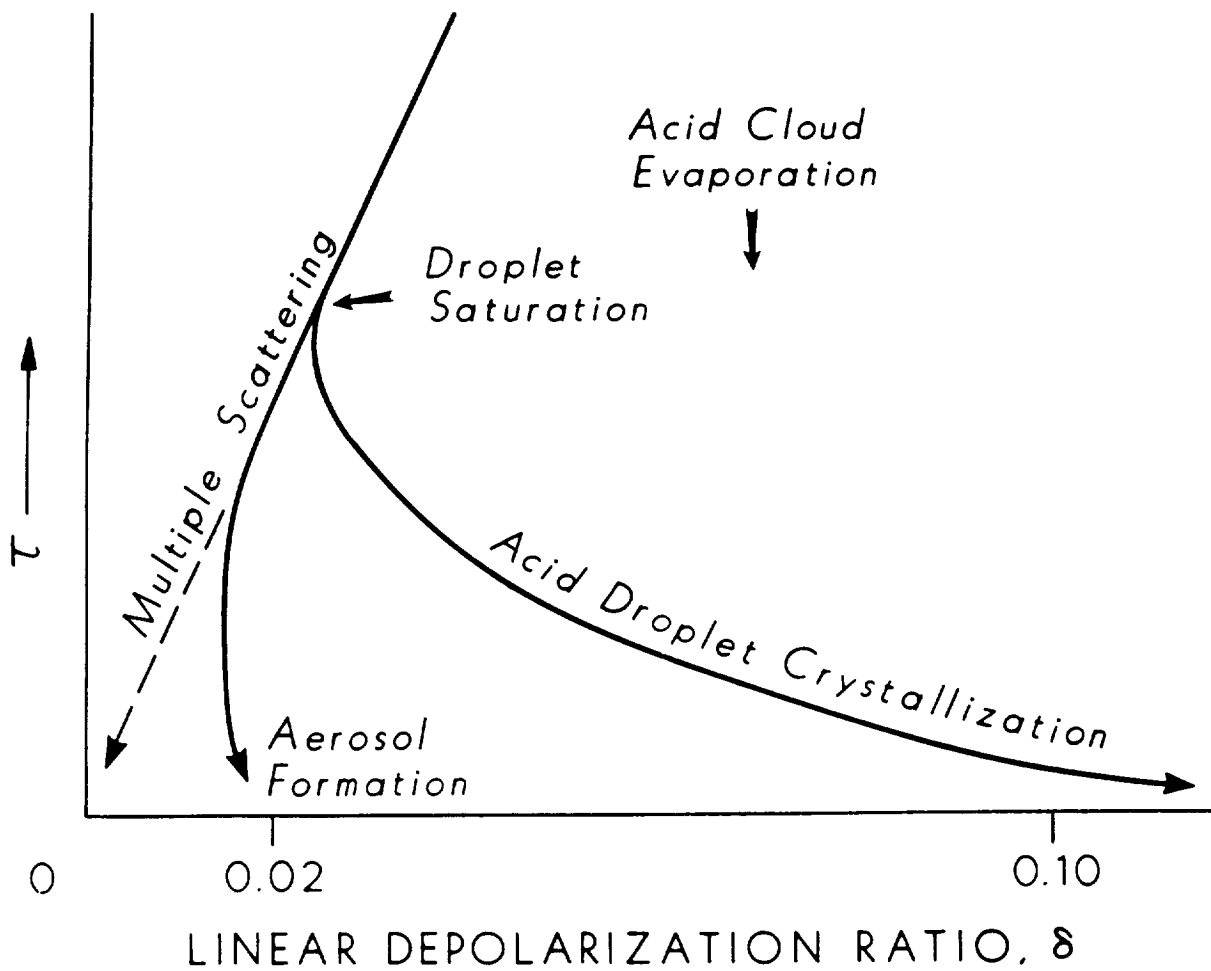


Fig. 5 A schematic portrayal of the depolarizing behaviors of evaporating acid droplet clouds. The largest δ values of ~ 0.10 - 0.15 are produced as saturated solution droplets crystallize into optically inhomogeneous and nonspherical particles.

induced depolarization on cloud optical thickness, as approximated by the straight dashed line approaching zero depolarization in Fig. 5. Interestingly, this behavior was not observed during our experiments for optically thin clouds derived even from pure water samples, probably as a result of the contamination from aerosols that were not cleansed from the chamber. The second path diverges slightly from that for pure drop evaporation owing to the final formation of a dry aerosol particle. It is assumed that this aerosol is composed predominantly of minute ammonium sulfate particles formed from natural ammonia gas reactions during the course of the cloud experiments. Although these particles are probably crystalline and nonspherical, depolarization ratios only on the order of a few percent, or roughly equivalent to that of a pure molecular atmosphere, are produced due to their small sizes relative to the laser wavelength. Finally, as a result of reaction product formation in a saturated solution drop, a third depolarization path in which δ values reach $-0.10-0.15$ is possible. We conclude that these higher linear depolarizations are caused by partially crystallized, mixed-phase particles that are both inhomogeneous and nonspherical. The δ values initially increase during evaporation as a result of continued reaction product formation and the growing importance of the crystallized material in determining the backscattering properties. Previous laser studies of inhomogeneous drop backscattering¹³ have shown that depolarization is generated by the scattering of suspended matter within a spherical drop, particularly when the material interferes with the axial reflection off the rear drop surface. At later stages of evaporation, we believe that the droplet becomes nonspherical with an irregular water coating on the crystalline material. This final stage is analogous to the melting of snowflakes in the atmosphere, which has been shown to produce an increase in depolarization.¹⁴

Although it is difficult to obtain reliable in situ cloud samples of such

small and volatile particles, the photomicrograph of Fig. 6 shows cloud particles collected on the same slide about 3-4 min and 15-17 min after ammonia gas was injected into a sulfuric acid cloud. Represented are crystalline particles displaying a hexagonal symmetry that are surrounded by a "halo" of evaporated acid solution products, and also micron-sized ammonium sulfate particles that appear to have been collected as dry aerosols. Although it is not always clear whether the crystalline materials are an evaporation product formed on the slide or while suspended in an acid drop, it is reasonable to assume that reaction products will begin to dominate the backscattering properties of the droplets at some point during the evaporation process.

To extend these acid drop crystallization findings to the problem of determining the nature of stratospheric clouds, it is of course necessary to consider the availability of ammonia gas and the sulfuric acid droplet residence times in the stratosphere. Although a rigorous examination of this issue is beyond the scope of the current investigation, the long residence times of volcanically-injected aerosols of from a few to several months in the stratosphere would favor reaction product formation. Since atmospheric ammonia is largely a product of biological activity and pollution emissions at the earth's surface, gaseous diffusion across the tropopause represents the source of ammonia normally entering the lower stratosphere. (Although ammonia gas may accompany other volcanic volatiles injected into the stratosphere, photo-oxidation and acid cloud formation processes would probably rapidly consume this material.) Thus acid droplet crystallization effects would be most likely observed at the base of stratospheric cloud layers, where acid droplets are evaporating and ammonia gas is relatively abundant.

The range of δ values we have obtained in the laboratory for simulated aerosols compares favorably with several polarization lidar observational

ORIGINAL PAGE IS
OF POOR QUALITY

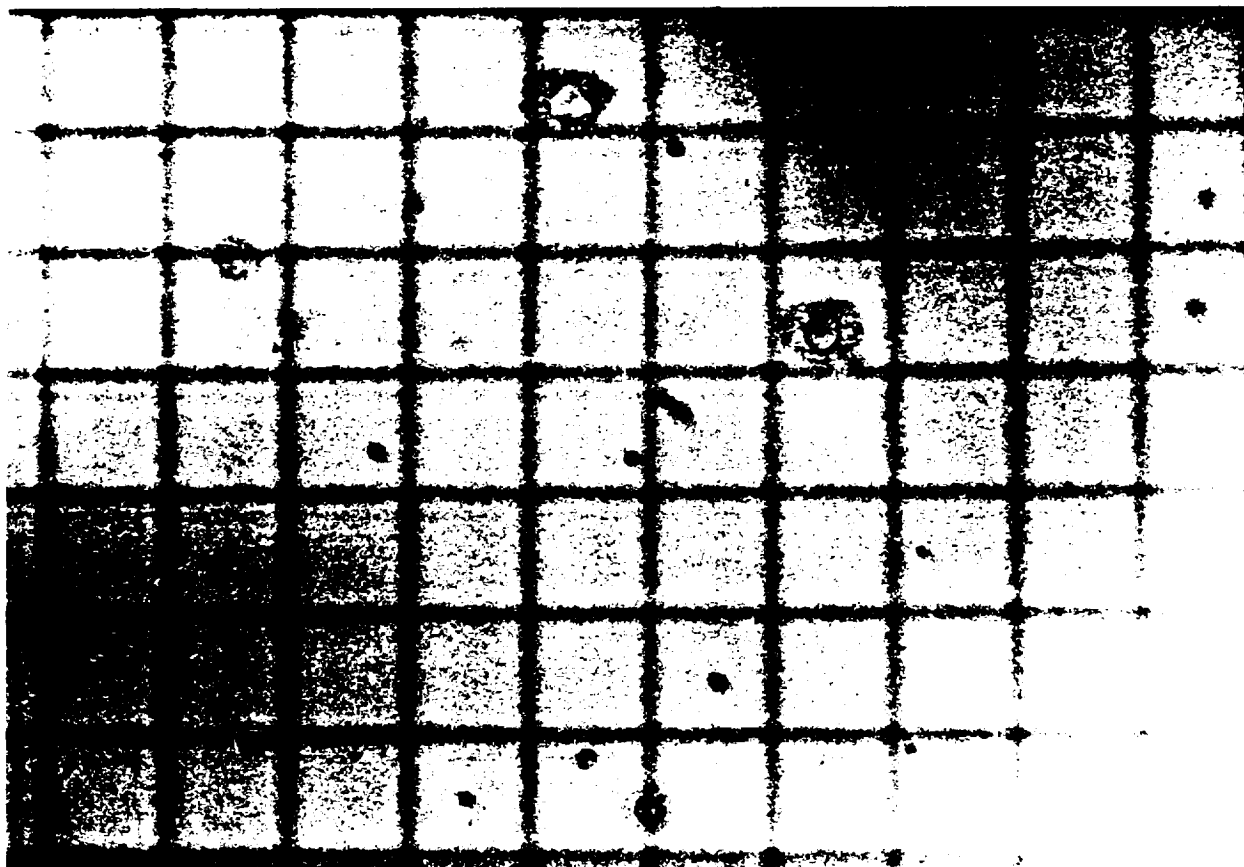


Fig. 6 Typical photomicrograph of cloud samples obtained by sedimentation following ammonia gas injection into an evaporating acid cloud, showing the deposition of both wet and dry crystalline particles. Each grid box is $\sim 10 \mu\text{m}$ on a side.

studies of stratospheric clouds. The data of Iwasaka and Hayashida⁴ are particularly interesting in that depolarization observations spanning about an 11-week period following the May 1980 Mount St. Helens eruption are reported. At two weeks after the eruption, a rather strongly scattering cloud displaying δ values of -0.01 to 0.03 (at the cloud peak) was sampled. The gradual decay and descent of the cloud layer was accompanied by much higher lidar δ values in the lower cloud/tropopause region, including $0.4-0.6$ and $0.06-0.07$ at about 10 and 11 weeks, respectively. These lidar observations are consistent with the single and multiple backscattering behavior of sulfuric acid droplet clouds, and with ice crystal and partially crystallized acid droplet scattering in the lower stratosphere as the cloud diminished, respectively.

Polarization measurements in the Antarctic stratosphere⁶ provide data that are again in agreement with strongly depolarizing ice cloud scattering, non-spherical aerosols with $-0.06-0.10$ δ values, and spherical homogeneous droplets displaying $\delta = 0.01$. Interestingly, the $-0.06-0.10$ δ values were measured in a relatively strongly scattering cloud layer just prior to a backscatter enhancement event caused by ice crystals. Nearly coincident balloon measurements indicated the unusually large concentration of 15 cm^{-3} for particles larger than $0.3 \text{ }\mu\text{m}$ in diameter. Since the lidar depolarization and particle size data would appear to be consistent with our laboratory measurements, it follows that partially crystallized sulfuric acid droplets could have been detected, although the connection of these particles to the subsequent appearance of ice crystals is not clear. It is possible, for example, that at cold stratospheric temperatures completely crystallized particles may serve as ice nuclei, or that ice crystals form from growing acid droplets that freeze after dilution, as suggested by Steele et al.¹⁵

Finally, in support of the view that partially crystallized acid droplets

are indeed a good candidate for explaining an unknown class of stratospheric aerosols, we note that lidar data collected during the post-El Chichon eruption period by Kobayashi et al.¹⁶ show a tendency for δ values to increase with decreasing values of the scattering ratio. Peak δ values of -0.05 - 0.07 were measured in weakly scattering layers (scattering ratio $R \leq 5$), although as they pointed out, the depolarization measurements include molecular scattering effects and so underestimate (by a factor of ~ 1.5 according to our analysis) the depolarization generated by the aerosol component alone. Ice crystal scattering effects are unlikely to be responsible for their findings, whereas acid droplet evaporation and subsequent partial crystallization would likely produce a similar tendency and peak δ values. Thus we consider it worthwhile to pursue modeling studies to determine the importance of ammonia gas reactions as a sink for stratospheric sulfuric acid clouds.

This research was supported by NASA Grant NAG-1-686, and recent laboratory system improvements were funded by NSF Grant ATM85-13975. The authors wish to thank J. Alvarez for his contributions to the experimental plan.

References

1. Russell, P.B. and R.D. Hake, "The post-Fuego stratospheric aerosol: Lidar measurements, with radiative and thermal implications. *J. Atmos. Sci.* 34, 163 (1977).
2. Pollock, J.B. and C.P. McKay, "The impact of polar stratospheric clouds on heating rates of the winter polar stratosphere. *J. Atmos. Sci.* 42, 245 (1985).
3. Poole, L.R. and M.P. McCormick, "Polar stratospheric clouds and the Antarctic ozone hole," *J. Geophys. Res.* 93, 8423 (1988).
4. Iwasaka, Y. and S. Hayashida, "The effects of the volcanic eruption of St. Helens on the polarization properties of stratospheric aerosols: Lidar measurements at Nagoya," *J. Meteor. Soc. Japan* 59, 611 (1981).
5. Kent, G.S., L.R. Poole and M.P. McCormick, "Characteristics of arctic polar stratospheric clouds as measured by airborne lidar," *J. Atmos. Sci.* 43, 2149 (1986).
6. Iwasaka, Y., "Large depolarization ratio of the winter Antarctic stratospheric aerosol layer: Lidar measurement at Syowa Station (69° 00'S, 39° 35'E), Antarctica," *J. Meteor. Soc. Japan* 64, 303 (1986).
7. Poole, L.R., M.T. Osborn and W.H. Hunt, "Lidar observations of arctic polar stratospheric clouds, January 1988: Signatures of small, solid particles at temperatures above the frost point," *Geophys. Res. Lett.* (in press).
8. Reiter, R.H., H. Jager, W. Carnuth and W. Funk, "The stratospheric aerosol layer observed by lidar since October 1976: A contribution to the problem of hemispheric climate," *Arch. Met. Geophys. Biokl.* 27, 121 (1979).
9. Sassen, K., "Depolarization of laser light backscattered by artificial clouds," *J. Appl. Meteor.* 13, 923 (1974).

10. Sassen, K. and R.L. Petrilla, "Lidar depolarization from multiple scattering in marine stratus clouds," *Appl. Opt.* 25, 1450 (1986).
11. Pal, S.R. and A.I. Carswell, "Polarization anisotropy in lidar multiple scattering for atmospheric clouds," *Appl. Opt.* 24, 3464 (1985).
12. Rubel, G.O. and J.W. Gentry, "Onset of particle crystallization resulting from acid droplet ammonia gas reactions," *J. Aerosol Sci.* 18, 23 (1987).
13. Sassen, K., "Optical backscattering from near-spherical water, ice and mixed phase drops," *Appl. Opt.* 16, 1332 (1977).
14. Sassen, K., "Laser depolarization 'bright band' from melting snowflakes," *Nature* 225, 316 (1975).
15. Steele, H.M., P. Hamill, M.P. McCormick and T.J. Swisler, "The formation of polar stratospheric clouds," *J. Atmos. Sci.* 40, 2055 (1983).
16. Kobayashi, A., S. Hayashida, Y. Iwasaka, M. Yamoto and A. Ono, "Consideration of depolarization ratio measurements by lidar-in relation to chemical composition of aerosol particles," *J. Meteor. Soc. Japan* 65, 303 (1987).